JOURNAL OF CATALYSIS 26, 175–190 (1972)

Quantitative Infrared Spectroscopy of Amines in Synthetic Zeolites X and Y

I. Alkylammonium Y Zeolites as Precursors of Acid Hydroxyls in Deaminated Zeolites Y

P. A. JACOBS AND J. B. UYTTERHOEVEN

Centrum voor Oppervlaktescheikunde en Colloïdale Scheikunde, De Croylaan 42, B-3030 Heverlee, Belgium

Received July 20, 1971

Na^+ ions in zeolite Y have been replaced by the following alkylammonium ions: mono-, di-, and trimethylammonium, mono-, di-, and triethylammonium, propyl-, isopropyl-, and butylammonium, piperidinium and pyridinium. The interaction of the zeolite lattice with the ions has been investigated by infrared spectroscopy. A comparison was made between the ∂NH^+ and ∂CH frequencies of these ions in the zeolite and the corresponding frequencies in alkylammonium halogenides. Frequency shifts were correlated with structural properties of the zeolite.

The zeolites were deaminated by heating in anhydrous conditions, and the creation of hydroxyl groups followed by scanning the hydroxyl stretching spectra. Deamination of the primary alkylammonium zeolites produced a stoichiometric hydrogen Y zeolite. With the secondary and tertiary ions considerable dehydroxylation was observed. The decomposition mechanisms of the ions are discussed.

The special behavior of the pyridinium zeolite suggests that the 3550 cm^{-1} hydroxyl band contains several components. Decomposition of the pyridinium ions results in a dehydroxylated zeolite containing Lewis acid sites of different strength.

INTRODUCTION

Several publications have appeared dealing with the thermal decomposition of ammonium ions in NH_4^+–Na^+Y zeolites (*1–5*). For heat treatments below 500°C, a simple decomposition mechanism of the NH_4^+ ions has been proposed involving the evolution of ammonia and the creation of hydroxyl groups. This mechanism is as follows:

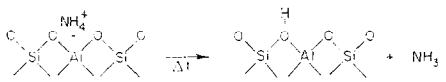

The product obtained is commonly called hydrogen Y zeolite (HY). The infrared spectra of HY zeolite contain stretching vibration bands of these hydroxyls at around 3650 cm^{-1} and 3550 cm^{-1}. The high frequency (HF) band around 3650 cm^{-1} is generally assigned to hydroxyls formed with the O_1 type oxygens (*6–8*). The low frequency (LF) band around 3550 cm^{-1} is asymmetric, and attributed to hydroxyls formed with oxygens belonging to the cages of the cubooctahedron (*3, 4, 9*), with a preferential location at the O_3 type oxygens (*10, 11*). Heating at higher temperatures produces dehydroxylation.

Products with quite different properties can be obtained by calcination of the NH_4^+–Na^+Y system under different conditions (*13, 14*). Sample geometry and packing, and as a consequence the partial pressure of the decomposition products

water and ammonia, play an important role in determining the nature of the end products. Only thoroughly outgassed samples, slightly packed in a shallow bed, or thin zeolite wafers used in infrared work (*2–5, 15, 16*) can produce the typical HY samples. Heating under so-called deep-bed conditions produces partially dehydroxylated samples. These are distinguished from the HY samples by an increased thermal stability and a hydroxyl spectrum which is different in many aspects from that of a HY sample (*17, 18*).

We tried to produce hydroxyls in Y zeolites by the thermal decomposition of samples saturated with different alkylammonium ions. The aim of the work was to investigate the influence of the different types of ions on the creation of hydroxyls and their distribution over the two hydroxyl bands. Since this work was started, the decomposition of a tetramethylammonium Y zeolite was studied by Wu *et al.* (*20*). IR, DTA and TGA methods were used in that work together with a careful analysis of the gaseous decomposition products. It was shown that the decomposition of tetraalkylammonium ions is more complex than a simple deamination. The mechanism of decomposition of alkylammonium ions in zeolite Y will also be discussed in this paper.

Experimental Methods

Materials

The Union Carbide Corp., Linde division, supplied synthetic zeolite Y (SK-40, lot No. 5135). To avoid Na^+ deficiency the sample was treated with 2 *N* NaCl solution at 60°C and washed free of excess salt. Using standard analytical methods the anhydrous unit cell composition was found to be $Na_{55}(AlO_2)_{55}(SiO_2)_{137}$. The SiO_2/Al_2O_3 ratio was 5.02.

The sodium zeolite was treated with 1 *N* solutions of alkylammonium chlorides, shaken overnight, centrifuged and washed with distilled water. This treatment produced the end members of the exchange isotherms, described by Theng, Vansant and Uytterhoeven (*19*). The anhydrous unit cell composition of these samples is given in Table 1. The alkylammonium zeolites were dried at 30°C and stored over a saturated NH_4Cl solution in order to ensure a constant weight basis. The different samples will further be indicated by the initials of the saturating alkylammonium ions as used in Table 1.

For spectroscopic examination, an aliquot of the samples was slightly ground. Thin films were prepared by compacting 20 to 40 mg of powder without binder between

TABLE 1
Chemical Composition of the Zeolites

Anhydrous unit cell composition			Maximum exchange	
			%	meq/g
Na_{55}	$(AlO_2)_{55}(SiO_2)_{137}$	NaY	100	4.34
$(NH_4)_{38.5}Na_{16.5}$	$(AlO_2)_{55}(SiO_2)_{137}$	Ammonium	70	3.04
$(M1)_{37.5}Na_{17.5}$	$(AlO_2)_{55}(SiO_2)_{137}$	Methylammonium	68	2.95
$(E1)_{36.5}Na_{18.5}$	$(AlO_2)_{55}(SiO_2)_{137}$	Ethylammonium	66	2.86
$(P1)_{33.5}Na_{21.5}$	$(AlO_2)_{55}(SiO_2)_{137}$	Propylammonium	61	2.65
$(IP)_{28}Na_{27}$	$(AlO_2)_{55}(SiO_2)_{137}$	Isopropylammonium	51	2.21
$(B1)_{29}Na_{26}$	$(AlO_2)_{55}(SiO_2)_{137}$	Butylammonium	53	2.30
$(M2)_{30}Na_{25}$	$(AlO_2)_{55}(SiO_2)_{137}$	Dimethylammonium	55	2.39
$(E2)_{22}Na_{33}$	$(AlO_2)_{55}(SiO_2)_{137}$	Diethylammonium	40	1.74
$(M3)_{24}Na_{31}$	$(AlO_2)_{55}(SiO_2)_{137}$	Trimethylammonium	44	1.91
$(E3)_{14}Na_{41}$	$(AlO_2)_{55}(SiO_2)_{137}$	Triethylammonium	26	1.13
$(PY)_{38.5}(Na)_{16.5}$	$(AlO_2)_{55}(SiO_2)_{137}$	Pyridinium	70	3.04
$(PI)_{26.5}Na_{28.5}$	$(AlO_2)_{55}(SiO_2)_{137}$	Piperidinium	48	2.09

two steel dies. The load was about 900 kg/cm^2 of film.

Spectroscopic Conditions

Disks of 2 × 2 cm containing 5–8 mg of material/cm^2 of film were introduced in a vacuum infrared cell. This cell was described in previous work (*3*). The spectra were recorded on a Beckman IR-12 grating spectrometer, in the bending zone between 1300 and 1700 cm^{-1} and in the stretching zone between 2600 and 4000 cm^{-1}. All the spectra were scanned at room temperature. The slit setting of the instrument was such that the resolution was better than 1.5 and 3.5 cm^{-1} in the bending and stretching zones, respectively.

Procedures

The disks in the cell were evacuated at room temperature by pumping to a dynamic vacuum of 10^{-6} Torr for at least 2 hr. The temperature was raised at a rate of 12°C min^{-1} to about 125°C under continuous evacuation and maintained for about 2 hr. The sample was then cooled to room temperature and a spectrum was recorded. This operation was followed by similar steps with outgassing at 225, 350, and 450°C.

After each stage of outgassing several spectra were taken in the hydroxyl stretching region. The background was eliminated by tracing a straight base line tangent to the spectra at 3800 and 3350 cm^{-1}. Overlapping of the two hydroxyl bands was resolved graphically. The band areas were determined using a rolling disk planimeter. From these band areas absolute hydroxyl concentrations were obtained with the integrated form of the Beer-Lambert law as used by Hughes and White (*15*):

$$B = cl\int \epsilon_\nu^{(a)}\, d\nu = \int \log(T_0/T)_\nu\, d\nu,$$

in which B is the integrated absorbance of a peak (cm^{-1}), l the film thickness (mg dry zeolite/cm^2 of wafer), c the concentration of absorbing species (mEq/g of dry zeolite). $\epsilon_\nu^{(a)}$ is the apparent molar extinction coefficient at frequency ν, and $\int \epsilon_\nu^{(a)}\, d\nu$ is the apparent integrated absorption intensity (cm mole^{-1}). For the high frequency (HF) and low frequency (LF) bands the integrated intensities 5.281 and 3.525 cm μmole^{-1} were used, respectively. These were obtained after conversion of the extinction coefficients obtained in earlier work (*3*).

In the deformation region overlapping of the different modes could not be eliminated graphically. Therefore the spectra were resolved in a Dupont curve resolver using the appropriate analytical functions of the important bands. These functions were established by using the criterion of Abramowitz and Bauman (*21*) for measuring the relative amount of Lorentzian and Gaussian character of a band. The band area was calculated numerically using Simpson's rule, and further used in the integrated Beer-Lambert law. The error of this procedure, including all the experimental steps is estimated to be lower than ±3.5%.

Characterization of the Decomposition Products

The decomposition of the samples M2 and B1 was followed in a Mettler thermoanalyzer coupled to a Balzer type QM6101 quadrupole mass spectrometer. TGA, DTA and gas analysis data were recorded simultaneously while the samples were heated at a rate of 4°C min^{-1} under high vacuum.

Results

1. *The Vibration Frequencies and Their Assignment*

The spectrum of the alkylammonium ions is easily influenced by intermolecular interactions. Therefore the assignment of the different bands can only be made by a careful comparison with the literature data. In the stretching zone only the CH bands are well defined, but the strong absorption of the NH groups is broad and very diffuse.

The bending frequencies of all the samples are listed in Table 2 together with the assignments. These are based on a comparison with the spectra of the corresponding amines, alkylammonium halide salts, and with the assignment made in earlier work for amines or alkylammonium ions adsorbed on clays or zeolites. The primary

TABLE 2
ASSIGNMENT OF THE DEFORMATION MODES[a]

Sample: Assignment	M1Y (*1,2,3*)[b]	M2Y (*1,3,4*)[b]	M3Y (*1,4*)[b]	E1Y (*3,5,6,7*)[b]	E2Y (*3,5,6*)[b]	E3Y (*8*)[b]	P1 (*9*)[b]	IP	B1 (*9*)[b]	Band envelope
ν_2H_2O	1640 sh	1640 sh	1640 s[c]	1640 sh	1640 sh	1640 s[c]	1640 sh	1640 sh	1640 sh	—
∂NH_3^+as	1620 vs			1620 vs			1620 vs	1625 vs	1625 vs	G
∂NH_2^+sciss.		1625 vs			1615 vs					G
∂NH_3^+sym	1545 vs			1540 vs			1533 vs	1535 vs	1533 vs	G
∂CH_3as	1505 sh[d]	1470 vs	1485 s	1462 s[e]	1460 s[e]	1450 s[e]	1462 s[e]	1475 s	1455 sh[e]	L
	1470 s[d]	1440 sh	1460 sh							
∂CH_2ang				1480 s[e]	1480 s[e]	1477 s[e]	1475 s[e]		1467 vs[e]	L
∂NH^+			1425 w			1435 m				G
∂NH_x^+wagg	1425 m	1420 w								G
∂CH^3sym	—	—	—	1402 s	1400 m	1390 m	1397 m	1407 s[f]	1385 m	L
								1392 s[f]		

[a] sh = shoulder; vs = very strong; s = strong; m = medium; w = weak; G = Gaussian, L = Lorentzian shape.

[b] *1.* Bellanato, J., *Spectrochim. Acta* **16,** 1344 (1960); *2.* Cabana, A., and Sandorfy, C., *Spectrochim. Acta* **18,** 843 (1962); *3.* Fripiat, J. J., Pennequin, M., Poncelet, G., and Cloos, P., *Clay Miner.* **8,** 119 (1969); *4.* Ebsworth, E. A. V., and Sheppard, N., *Spectrochim. Acta* **18,** 843 (1962); *5.* Chenon, B., and Sandorfy, C., *Can. J. Chem.* **36,** 1181 (1958); *6.* Farmer, V. C., and Mortland, M. M., *J. Phys. Chem.* **69,** 683 (1965); *7.* Herzberg, G., "Infrared and Raman Spectra of Polyatomic Molecules," 11th printing, p. 360. Nostrand, New York; *8.* Sauvageau, P., and Sandorfy, C., *Can. J. Chem.* **38,** 1901 (1960); *9.* Fripiat, J. J., Servais, A., and Leonard, A., *Bull. Soc. Chim. Fr.* 635 (1962); *10.* Bellamy, L. J., "The infrared spectra of complex molecules," 2nd ed. Wiley, London, 1958.

[c] This band completely disappeared at 200°C: it is therefore the ν_2 band of adsorbed water.

[d] Two bands produced by the splitting of the doubly degenerate vibration ν_{10} (E) (*1*).

[e] The CH_2 def. mode gives rise to absorption close to 1465 cm^{-1} and CH_3 as. def. to 1450 cm^{-1}. Variations of more than 20 cm^{-1} only with strongly electronegative atoms (*10*).

[f] Splitting of the CH_3 sym. def. mode allows identification of branched-chain systems (*10*).

alkylammonium–zeolite complexes are all characterized by both the symmetric (~1545 cm^{-1}) and asymmetric (~1625 cm^{-1}) bending modes of the $-NH_3^+$ groups. The secondary derivatives have the $-NH_2^+$ scissoring mode (~1620 cm^{-1}), while the tertiary show the $-NH^+$ deformation band (~1430 cm^{-1}). Our assignments are in agreement with those proposed by Fripiat *et al.* (*22*) for alkylammonium montmorillonites.

Our spectra of the PIY sieve are essentially the same as the spectrum published by Hughes and White (*15*) for piperidine adsorbed on a hydrogen Y zeolite at 150°C.

For the PY sample we adopted the assignments originally given by Parry (*25*) and by Basila, Kantner and Rhee (*26*) for pyridine adsorbed on oxides. The spectrum of our PY zeolite is given in Fig. 1, after pretreatments at increasing temperatures. The band around 1550 cm^{-1} is the ν_{19b}, typical for pyridinium ions. The band at 1455 cm^{-1} is the same ν_{19b} vibration for pyridine. The ν_{19a} band occurs at 1490 cm^{-1}. Our spectra show that at room temperature only pyridinium is present. At increasing temperatures a band develops at 1455 cm^{-1} indicating the presence of coordinately held pyridine. The shoulders clearly present in the ν_{19b} band, at 1550 and at 1455 cm^{-1} as well, is discussed below. The νN^+H (ν_{7a}) band is observed at 2190 cm^{-1}.

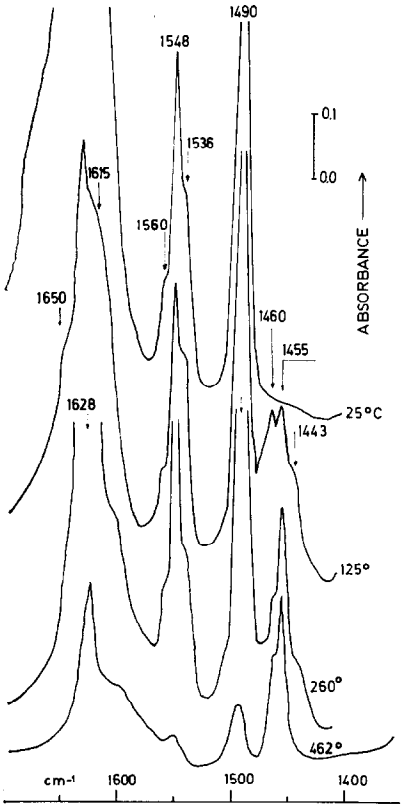

FIG. 1. Room temperature spectra of the pyridinium Y zeolite at increasing outgassing temperatures.

It is important to notice that all the NH deformation bands for the aliphatic ions have an almost pure Gaussian shape, while the CH deformations produce pure Lorentzian bands (Table 2).

2. *Influence of Pretreatment Temperature on the Spectra*

Heating the samples in vacuum results in a deamination reaction: the NH and CH bands decrease in intensity. For the δNH_3^+ sym. a shift upwards of about 10–12 cm^{-1} was observed on heating to 200°C. Two hydroxyl bands appear around 3650 and 3550 cm^{-1}.

These hydroxyls are identical to those in HY zeolites generated by decomposition of NH_4^+Y. This similarity is deduced from the frequency, the shape of the bands, and the reactivity of the hydroxyls towards ammonia and pyridine. Adsorption of NH_3 or pyridine results in a decrease of the intensity of both bands in a way consistent with the behavior of HY as described in the literature (*8*). When pyridine is adsorbed at 150°C, bands appear in the spectrum at 1547 and at 1455 cm^{-1} typical for Brønsted and Lewis pyridine. The band at 1455 cm^{-1} is particularly intense on samples derived from secondary and tertiary alkylammonium or from the systems PI and PY, but is nonexistent on the samples derived from primary alkylammonium ions with the exception of E1.

3. *Change of the Hydroxyl Concentration with Pretreatment Temperature*

In Fig. 2 the total hydroxyl concentration (LF + HF) is plotted as a function of the outgassing temperature. As the

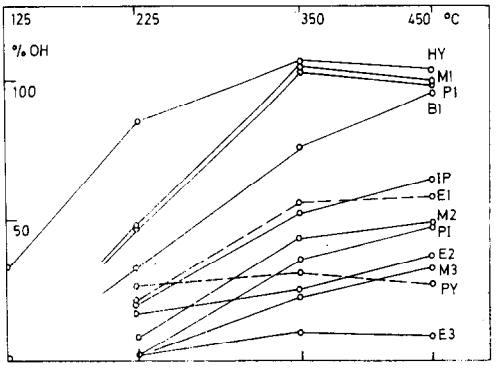

FIG. 2. Change of the total hydroxyl concentration in % of the possible amount as a function of the treatment temperature.

amount of organic ions is not the same for the different samples, the OH concentration is given in percentage of the maximum possible value, assuming that each organic ion could generate a proton. Figure 2 indicates that the decomposition is shifted to higher temperatures when the chain length increases, and when the ion becomes larger: this is deduced from the relative position of the points at 225°C. Only the primary alkylammonium ions, with the exception of E1, produce a hydroxyl content corresponding to 100%. For the other systems there is a considerable dehydroxylation which seems to be related to the complexity of the ions. The slope of curve PY in Fig. 2 indicates that the dehydroxylation proceeds from 225°C onwards, and probably starts at still lower temperatures.

The overall stoichiometry of the deamination reaction is further evidenced in Fig. 3 where the maximum OH content is plotted as a function of the amount of organic ions. For the primary ions, including ammonium but not E1, all the points are on the diagonal line, indicating that each organic ion generated one hydroxyl group. For all the other systems the points fall below the diagonal line: the vertical distance to that line indicates the extent of dehydroxylation. A confirmation of the 1:1 deamination reaction of the primary alkylammonium ions, and the dehydroxylating effect of the more complex ions, was obtained by converting the intensities of

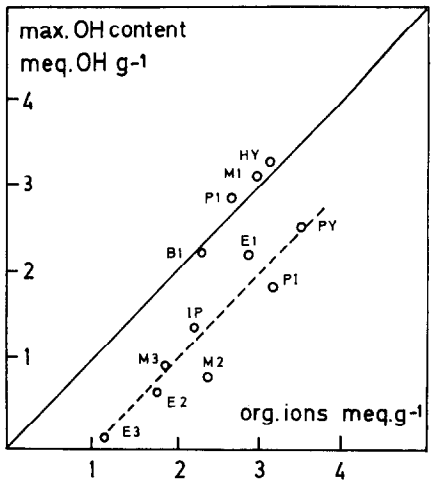

FIG. 3. The maximum hydroxyl concentration against the original concentration of the organic ions on the zeolite in the same units.

the νOH, ∂NH and ∂CH bands into concentrations, and by comparing the decrease of the latter two bands to the increase of the hydroxyl concentration. From the absence of NH bands we conclude that the decomposition of the organic ions was completed at 450°, although some carbonated organic material was sometimes left on the samples. For the sample PY, bands characteristic of coordinatively bonded pyridine but not of pyridinium were still present at that temperature.

4. Relative Intensities of the HF and LF Hydroxyl Bands

In HY zeolites the relative intensity of the LF and HF bands is a function of the amount of NH_4^+ ions present in the NH_4^+–NaY sample prior to the activation. This has been shown by several authors (*3*, *27*, *28*). To test the preferential development of the two types of bands in the alkylammonium zeolites, the ratio of the two bands, after conversion to concentration units, has been followed as a function of temperature (Table 3). Two factors influence the relative intensities of these bands, namely, the preferential adsorption of the amines on the HF hydroxyls, and the difference in stability of the two types of OH group. From the LF/HF values at low pretreatment temperature, and the decrease of that

TABLE 3
LF/HF RATIO, AFTER CONVERSION INTO HYDROXYL CONCENTRATION, AS A FUNCTION OF PRETREATMENT TEMPERATURE

Sample	Treatment (°C) 225	350	450	HY at 350°C[a]
NH_4^+	2.51	3.36	3.29	3.36
M1	4.40	3.41	3.31	3.38
E1	4.87	3.62	3.41	3.28
P1	7.47	5.38	3.04	3.05
IP	4.22	4.07	2.95	2.58
B1	8.5	5.5	2.95	2.96
M2	6.43	2.76	2.42	2.76
M3	—	2.45	1.90	2.01
E2	—	3.02	2.30	1.97
PY	—	4.28	2.60	3.40
PI	4.78	3.14	1.37	3.38

[a] LF/HF ratio in HY derived from Na^+–NH_4Y zeolites with NH_4^+ contents close to the concentration of the alkylammonium ions in the different samples.

ratio with increasing temperature, we deduce that the hydroxyls of the HF band have a higher affinity for the amines than the OH in the LF band. In the special case of PY the LF band is at a maximum and the intensity of the HF band is still zero after heating at 225°C.

In Table 3 are included the LF/HF ratios of NH_4^+–NaY samples containing various amounts of NH_4^+ ions, comparable to the content of alkylammonium ions in our different samples, and outgassed at 350°C. If we compare these ratios to the LF/HF values of our present samples outgassed at 450°C we find comparable values. Only the PY and PI samples show a lower LF/HF ratio indicating a preferential and considerable dehydroxylation of the LF hydroxyls.

5. Behavior of the Pyridinium-Y Sample

The spectrum of the pyridinium Y zeolite taken after outgassing at room temperature shows a band at 1550 cm^{-1}. This band decreases with increasing temperature. At the same time a new band develops at 1455 cm^{-1}. In Fig. 1 it appears that both bands show a shoulder indicating the presence of subcomponents. The profile of these bands changes on treatments at higher temperatures which indicates that the intensity of the different subcomponents changes at different rates. A semiquantitative estimate of these changes was made. The peak height of the three components in each of the bands was followed at different temperatures.

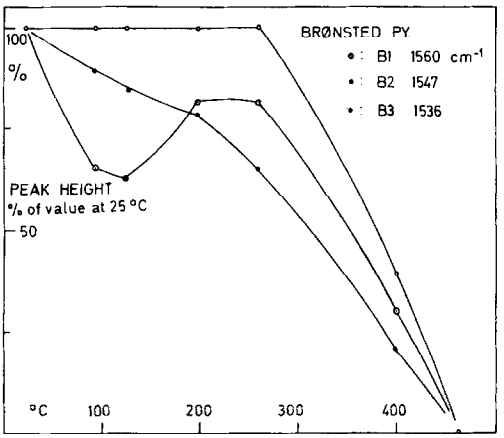

FIG. 4. Change of the different kinds of Brønsted bonded pyridine with the pretreatment temperature.

The intensity of the component at 1550 cm^{-1}, due to pyridinium ions, is given in Fig. 4 as a function of the pretreatment temperature. It is expressed in percentage of its intensity at room temperature. The central component at 1547 cm^{-1} (B2) remains unchanged up to 260°C, while both side components, at 1560 cm^{-1} (B1) and at 1536 cm^{-1} (B3), decrease in intensity even at low temperature. If this behavior is compared to that of the hydroxyl groups, it is evident that the LF OH band originates from the pyridinium ions involved in the B1 and B3 components, whereas the HF OH band is derived from the B2 pyridinium. If the different components reflect different locations of the pyridinium ions in the zeolite cages, we can anticipate that the LF OH band is the superposition of at least two components. The initial proportion of the components at room temperature is 1:4:3. The frequency of the B2 component can be compared to the frequency of pyridinium in the complex salt ($PYH^+ \cdot BF_4^-$), and the B3 component to pyridinium perchlorate (*23*).

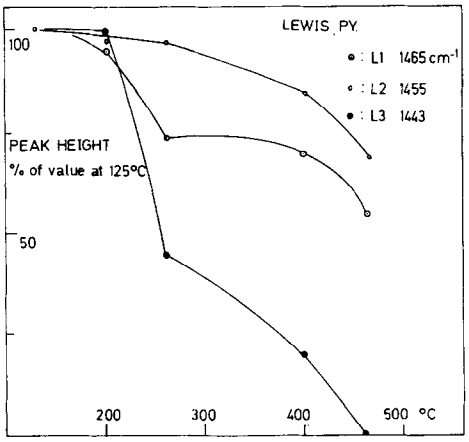

FIG. 5. Change of the different kinds of Lewis bonded pyridine with the pretreatment temperature.

The band at 1455 cm^{-1} is assigned to coordinately held pyridine. The height of the different peak components is plotted in percentage of their value at 125°C in Fig. 5. The frequency of the different components (L1 at 1465, L2 at 1455, and L3 at 1443 cm^{-1}) reflects the strength of interaction of the pyridine with the dehydroxylated sites. Similar frequencies were observed in the pyridine complexes with the Lewis acids BF_3, BCl_3 and BBr_3, respectively (*24*). The intensity of the L3 component decreases sharply above 200°C. Liengme and Hall (*29*) found a band at this frequency and ascribed it to pyridine coordinated to the residual Na^+ ions. The strongly held species (L1 and L2) are at an initial ratio of about 1:1 and resist very strong desorption procedures. After outgassing at 460°C the amount of pyridine still present was estimated to be between 10 and 20% of the initial amount of pyridinium ions.

6. *Characterization of Decomposition Products*

The IR results seem to indicate different decomposition mechanism for the primary alkylammonium ions and the other compounds. Therefore for two samples B1 and M2 a characterization of the decomposition products was made.

Figure 6 shows the infrared spectra of the solids in the CH stretching zone. At

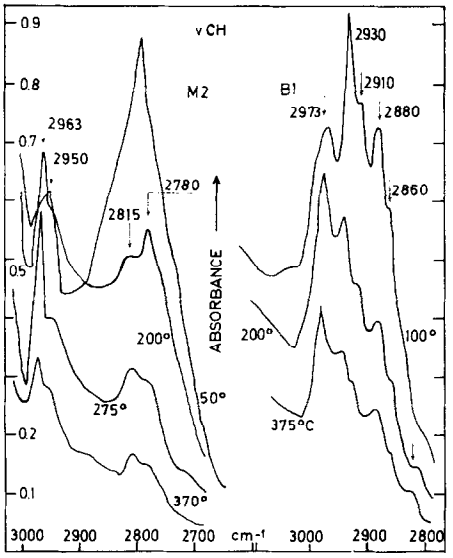

FIG. 6. νCH spectra of M2 and B1 zeolites: intermediate formation of alkoxy species.

increasing temperature components appear at 2973 and 2820 cm^{-1} in the B1 sample and at 2963 and 2815 cm^{-1} in the M2 sample. The bands first increase, reach a maximum around 375°C and then decrease. Wu, White and Venuto (*30*) observed the same two bands during the decomposition of tetramethylammonium offretite at 2950 and 2860 cm^{-1}, respectively. They assigned these bands to methoxy groups, and found support for their assignment in the spectra of methoxy intermediates on silica and alumina (*31*, *32*). In our samples the effect is more pronounced for M2 than for B1: assuming identical absorption coefficients many more alkoxy groups must be formed in M2 than in B1. The results obtained by TGA, DTA and gas analysis are given in Figs. 7 and 8. For the sample B1 water is released mainly below 250°C. The DTA and mass spectrometric results show two peaks at 90 and 150°C, characterized by endothermic temperature changes. Butylamine is evacuated in large amounts around 300°C, while above this temperature ammonia and butene are released. Two small endothermic events at 390 and 420°C are observed as H_2, propane, CO and CO_2 are evacuated.

For the sample M2 two water peaks

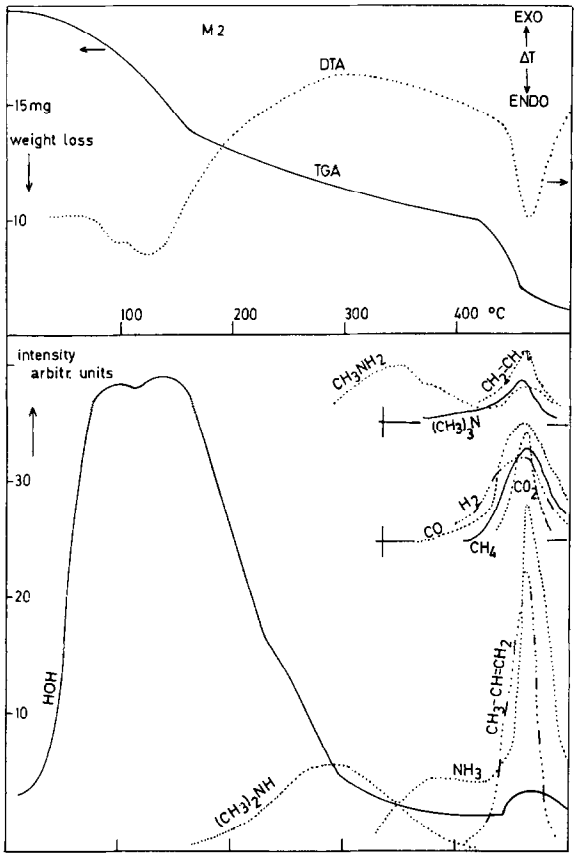

FIG. 7. DTA, TGA curves and products evacuated against temperature for sample M2.

and concomitant endothermic peaks are observed around 90 and 140°C. Dimethylamine molecules are released at 300°C. Above 350°C, ammonia and trimethylamine are evacuated. A sharp endotherm and the formation of high amounts of propylene and ammonia are observed at 460°C. At the same temperature significantly higher amounts of H_2, CO, CO_2 and CH_4 are evacuated as compared to the B1 sample. Small but significant amounts of ethylene are also detected.

DISCUSSION

1. *Interaction Between the Zeolite Lattice and the Organic Ions*

From the frequency shifts and band broadening of the νNH and ∂NH components (Table 2) we conclude that an intense hydrogen-bond interaction exists between the zeolite lattice and the organic ions. By a proper comparison with spectra of reference compounds, an estimate of the strength of this interaction can be made as shown below.

Normally infrared bands are Lorentzian shaped (*34*). From the fact that the ∂NH bands are Gaussian and the ∂CH bands are perfectly Lorentzian we can conclude that the hydrogen bonding affects the NH groups. This conclusion is also supported by the pronounced shift of these bands to higher wavenumbers (Table 4).

Because of strong band broadening and overlapping not much information is gained in the stretching region. Only for the pyridinium ions was the νNH^+ band clearly observed as an isolated band at 2190 cm^{-1}. Cook (*23*) studied the frequency decrease

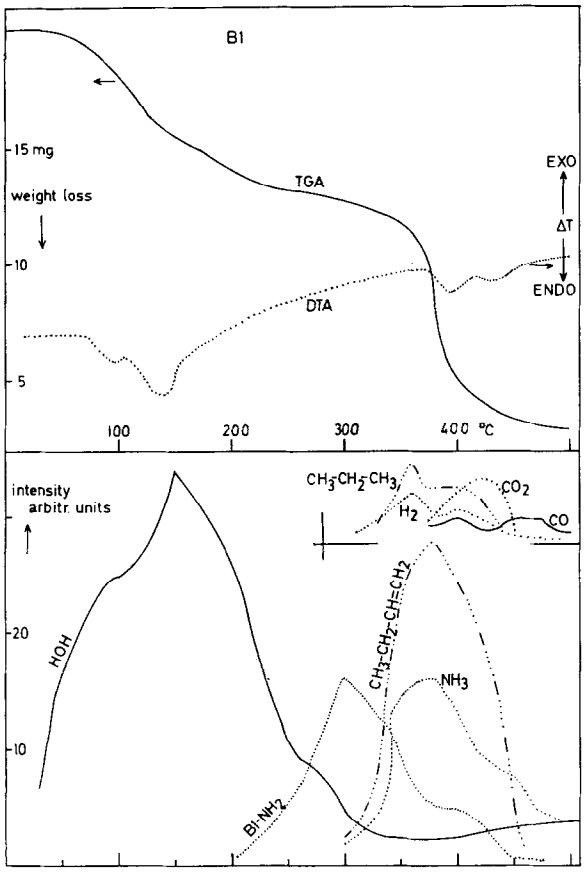

FIG. 8. DTA, TGA curves and products evacuated against the temperature for sample B1.

of this band in pyridinium halide salts. The NH^+ band was shifted to lower frequency following the sequence I^-, Br^- and Cl^-. This shift reflects the increasing force field exerted by these ions. If the wavenumber 2190 cm^{-1} observed in the PY sample is interpolated between Cook's data, the field exerted by the zeolite lattice on the organic ions is even stronger than the field of the Cl^- ions.

The ∂NH_3^+ symmetric band of the primary alkylammonium ions shifts upwards by hydrogen bonding. This vibration is at 1540–1533 cm^{-1} in zeolites (this work) at 1504 cm^{-1} in vermiculites (*35*) and at 1488 cm^{-1} in montmorillonites (*36*). This sequence reflects the charge density of the respective minerals and also the strength of interaction. A comparison of our work in zeolites with data on solid alkylammonium salts must take into account that the nature of the matrix has an influence on the frequency of the bands in salts. Therefore, for all our comparisons to solid salts, we selected literature data obtained in a KBr matrix. This condition limits the possibility of comparison because of the unavailability of reliable data for some vibrations. For the zeolite itself the nature of the binder had no effect: self-supporting films of zeolite and KBr disks gave the same spectra.

A comparison of the alkylammonium bending frequencies in zeolites and in the corresponding halides shows that the upwards shift in the zeolites is even stronger than in the chloride salts. This confirms the observations made with PY in the stretching region. Taking the frequencies of the chloride salts as a basis of comparison, we calculated the frequency shifts (Table 4). For most of the bands a posi-

TABLE 4
FREQUENCY SHIFTS OF SOME DEFORMATION BANDS WITH RESPECT TO THE SOLID HYDROCHLORIDE SALTS
$\Delta\nu^a = \nu_z^b - \nu_{Cl}$

∂NH_3^+ as.		∂NH_3^+ sym.		∂CH_2 ang.		∂CH_3 as.	
M1	42	M1	14	E1	3	M1	7
E1	15	P1	20	P1	4	M2	5
		B1	28	B1	−4	M3	4
B1	31			E3	−3	E3	−26
						P1	−6
						B1	−1

∂CH_3 sym.		∂NH^+		∂NH_2^+	
E3	−9	M3	7	P1	22
		E3	−13	E2	20

[a] The frequency shift in the zeolite w.r.t. the solid hydrochloride form; the latter are taken from the references in Table 2.

[b] Room temperature frequencies after room temperature outgassing. For ∂NH_3^+ the frequencies were determined on the spectra obtained after outgassing at 125°C.

tive shift is observed, particularly important for the N–H deformation.

For alkylammonium chloride salts Bellanato (*44*) observed a linear relation with positive slope between the frequency of different bending vibrations and the nucleophilic constant (n) of the anions of the salt matrix (Cl^-, Br^- and I^-). The nucleophilic constant measures the ability of the anions to donate electrons for hydrogen bonding: the n value decreases in the order I^-, Br^-, Cl^-. We looked for the same relation using literature data for different alkylamonium salts (Cl^-, Br^- and I^-) in the same matrix, and interpolated the frequencies obtained with zeolites on the scale of nucleophilic constants of the halogen ions. Support for the validity of the comparison is given by the compound E3 for which the method could be applied to the ∂NH^+ and ∂CH_2 modes giving n values of 3.80 and 3.66. With PY a value of 2.40 was obtained using the ν_{8b} bending vibration, whereas the interpolation of our data on the relation of Cook (*23*) for the N^+H (ν_{7a}) stretching mode produced a value of 2.15. The nucleophilic constant n for the zeolite obtained in this way cannot be considered to be an absolute value, since several factors contribute to the frequency shift. With the available literature data the values of Table 5 could be obtained.

TABLE 5
NUCLEOPHILIC CONSTANTS (n)[a]

Sample:	M1	E1	B1	E2	E3	PY
n	0.15	0.32	1.83	2.42	3.8	2.15

[a] The values are obtained from ∂NH_x^+ bands.

Systematic variations of these n values with respect to properties of the ions and of the zeolites are observed. Because of the ion sieve effects during the preparation of the samples (*19*), the number of organic ions in the different samples is variable from one alkylammonium ion to another. The n values of Table 5 are plotted as a function of the residual sodium ions in Fig. 9A. The increase of n with increasing amount of residual Na^+ ions indicates that the electrostatic energy contribution to the total energy of the hydrogen bond increases when the amount of residual Na^+ ions decreases.

The observed n values can also be correlated with characteristics of the ions. The

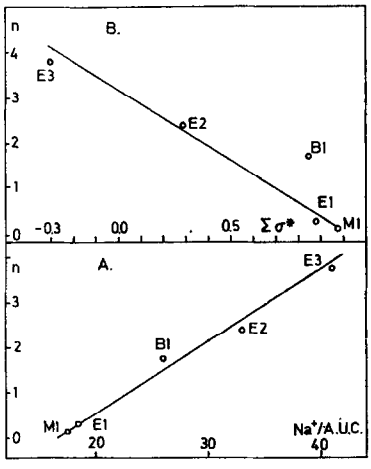

FIG. 9. Nucleophilic constants of the zeolite against the Taft factors of the cations (B) and against the residual Na^+ ions per anhydrous unit cell (A).

inductive effect of the alkyl groups in the ions also influences the hydrogen bonding. A quantitative expression for the inductive effect is given by the Taft factors σ^* (*37*). The relation between the Taft factors and the value n is given in Fig. 9B. The observed relation indicates that the electrostatic energy of the hydrogen bond decreases when the inductive power on the N center increases.

2. Nature of the Deaminated Zeolites

The thermal decomposition of NH_4^+–NaY zeolites produces typical HY zeolites when a rapid evacuation of the decomposition products is realized. In a "deep bed" calcination, prolonged contact with the decomposition products (NH_3 and/or H_2O) produces a hydrolysis which extracts aluminum from the lattice (*13*). Infrared spectroscopy can distinguish between the end products of both treatments.

The infrared spectra of our deaminated samples contain only the hydroxyls at 3650 and 3550 cm^{-1}, which can react with NH_3. Therefore we conclude that the deaminated products are essentially HY zeolites. From the OH band areas it is further concluded that the deamination reaction of zeolites saturated with NH_4^+ and primary alkylammonium ions, with the exception of E1, proceeds stoichiometrically. One OH group is created for each alkylammonium ion initially present. Decomposition of more complex systems produces a partially dehydroxylated material, but the ir spectra give no evidence for a hydrolytic reaction. Adsorption of pyridine on the deaminated products confirmed the conclusions drawn from the band intensities: products derived from primary alkylammonium ions adsorb pyridine and produce PYH^+, whereas the partially dehydroxylated samples contain sites where pyridine molecules are adsorbed as such. In the special case of decomposition of a pyridinium sample, the decrease of the pyridinium peak and the concomitant increase of a pyridine band demonstrates that the dehydroxylation mechanism takes place even at low temperature.

Wu *et al.* (*20*) report that the hydroxyl groups of the faujasite sample resulting from the TMAY (tetramethylammonium) system are thermally more stable than the OH groups of an ordinary HY. We have no data to confirm this since we confined all our measurements in the temperature region below 500°C. However, we estimated from Fig. 3 of their work the hydroxyl concentration of the TMA faujasite outgassed at 350°C, using our integrated intensities of the OH bands. The amount of hydroxyl was less than 50% of the maximum possible amount derived from the TMA content of the sample.

Our data for di- and trimethylammonium faujasites are in complete agreement with the data of Wu *et al.* (*20*).

Decomposition of TMA in offretite (*30*) generates OH bands at 3690, 3615 and 3550 cm^{-1}. Wu, White and Venuto interpret these bands as being due to hydroxyls identical in nature to those in HY zeolites, but shifted to somewhat higher wavenumbers. The shifts would reflect structural differences in HY and in offretite. We want to point out the similarity between the hydroxyls in that offretite sample, and those generated in NH_4^+Y samples deammoniated in conditions intermediate between deep and shallow calcination bed geometries. In such samples the hydroxyl spectrum is also intermediate between the spectrum of an HY and a deep bed calcined sample (*18*).

The rate of evacuation of the decomposition products is no doubt one of the major factors determining the nature of the end products of the calcination. Heating NH_4^+Y under continuous outgassing does indeed produce almost stoichiometric HY samples (*3*). Bolton and Lanewala (*5*) heated NH_4^+Y samples in a stream of dry air at 375°C and observed a 25% dehydroxylation. Heating without any evacuation under deep bed conditions produces hydrolyzed and Al-deficient samples (*13*, *17*, *18*). For obvious steric reasons the evacuation of the decomposition products of alkylammonium ions is slower than in NH_4^+Y: the prolonged contact at high temperatures could increase the probability of dehydroxylation, but the concentration of hy-

drolytic gases in the pores is probably low enough to prevent hydrolysis of the samples. Moreover, according to the analysis of the decomposition products (Figs. 7 and 8), H_2O vapor is only present below 300°C. This idea is consistent with the fact that the extent of dehydroxylation was found to be proportional to the size of the organic ions. The different behavior of TMAY and TMA offretite, investigated by Wu *et al.* (*20*) and Wu, White and Venuto (*30*) can also be understood in this way; considering the different pore sizes of the zeolites Y and offretite, the evacuation of the decomposition products must indeed be easier in Y zeolite than in offretite. Thus Y zeolites suffer dehydroxylation, whereas in the offretite the intracrystalline pressure is probably high enough to hydrolyze the sample. However, systematic experiments are required to confirm these speculations.

3. Preferential Development of HF and LF Bands

When NH_4Y zeolites are heated the HF and LF bands develop progressively. Except in cases where NH_4^+ deficiency was observed before any heating, it was never reported that one of the OH bands develops preferentially before the other (*2–4*, *16*). In the reverse reaction, the adsorption of ammonia, no selectivity for one kind of hydroxyl is observed (*2*, *3*). Pyridine is known to react preferentially with the HF band (*4*, *9*, *15*).

In our samples ion deficiency was not observed. The decrease of the LF/HF ratio with increasing temperature listed in Table 3 is due to a preferential decomposition of ions on particular sites in the zeolite structure. The HF band is generally attributed to hydroxyls formed with O_1 type oxygens. The evolution of LF/HF indicates a preferential interaction of the amines with the hydroxyls formed on O_1. This preferential interaction is still more pronounced with the secondary and with the tertiary derivatives. Even more evidence for site heterogeneity is found in the spectrum of PY where a triplet of bands around 1550 cm^{-1} was observed.

The oxygen ions of the cubooctahedron cage (O_2, O_3 and O_4) are possible sites for the LF hydroxyls with a certain preference for the O_3 type oxygens. This implies that LF hydroxyls can be at sites where they are not immediately accessible for reaction with amine molecules. When a hydroxyl is formed on an oxygen of the cubooctahedron by decomposition of an organic ion located on a site II, the proton can migrate towards a less accessible site and become unavailable for interaction with the amines. This is a first factor to explain the preferential development of the LF band.

Another factor could be in the location of the organic cation itself. This location is not known in detail. A maximum of 32 ions/unit cell can be located on sites II near six-rings of oxygen ions. The dimensions of these rings correspond closely to the dimensions of the triangular base of the $-NH_3^+$ group and could thus offer maximum possibility for hydrogen bonding to the primary amines. According to Mortier, Bosmans and Uytterhoeven (*40*) other possible sites are on four-rings of oxygen ions formed by two O_1 and two O_2 oxygens inside the large cavities. The geometry of the secondary and tertiary ammonium ions being not particularly adapted to the S_{II} sites, it is not excluded that these ions are preferentially located and most stable on these four-rings, preventing the HF band to be formed.

4. Repartition of Protons Over the Two Hydroxyl Sites

From Table 3 it is clear that at comparable Na^+ levels the LF band is a little more, and the HF band is somewhat less developed in the samples derived from M1, P1 or B1 compared to NH_4^+–NaY samples.

For the other samples the dehydroxylation phenomenon makes it difficult to judge the preferential development of LF and HF band. For samples outgassed at 450°C, the LF/HF ratios seem to reflect only the difference in residual Na^+ content of the different samples, despite the fact that the hydroxyls of the LF band are known to be more easily affected by dehydroxylation than the hydroxyls of the

HF band (*3*). However, at 450°C for completely deaminated samples, there must be a rapid averaging of the protons over LF and HF sites, and the distribution of the protons cannot be strongly influenced by the nature of the alkylamonium ions initially present.

Finally, the PY and PI samples, after outgassing at 450°C are considerably dehydroxylated and it is clear that the LF band is preferentially affected. Pyridine is a weak base; piperidine is known as a strong base. The similarity in behavior with respect to dehydroxylation of the samples PY and PI indicates that steric factors influencing the rate of evacuation are important factors for the dehydroxylation.

5. *Evidence for Site Heterogeneity in PY Samples*

The splitting of the ν_{19b} band around 1550 cm^{-1} into three components probably indicates a heterogeneity in ion location sites. The middle component (1547 cm^{-1}), with the highest intensity, resists thermal treatment best. On decomposition of the corresponding pyridinium species, the HF band develops. Probably these pyridinium ions were located at the four-ring sites. The pyridinium involved in the other components (1560 and 1536 cm^{-1}) produces the low frequency band. It is rather difficult to speculate on a subdivision of the organic ions, although the most probable location for the ions involved in the formation of the LF hydroxyls seems to be on sites II. However, this implies the existence of two energetically different sites II.

At relatively low temperature (125°C), the Brønsted pyridine starts to decompose and bands of so-called Lewis pyridine develop. The decomposition mechanism of the pyridinium at this low temperature probably involves an active contribution of the zeolite lattice, resulting in a dehydroxylation and the creation of very strong adsorption sites of the Lewis type. The Lewis pyridine is most stable to thermal treatment (450°C). At this temperature Brønsted pyridine is quantitatively decomposed.

The bands typical for Lewis pyridine are also differentiated into three components. According to Liengme and Hall (*29*) the component at 1443 cm^{-1}, which is most easily removed by evacuation, can be assigned to pyridine coordinated to residual Na^+ ions. However, only 16 Na^+ ions/unit cell are available in our samples. Interaction of these ions with pyridine would imply that they have migrated from the inaccessible sites I and I′ into the large cavities. Such a migration and reorganization of the Na^+ ions over sites I, I′ and II during the deammoniation of NH_4^+–NaY has been observed. Gallezot and Imelik (*41*) located 50% of the residual Na^+ ions on sites II, whatever the Na^+ content of the sample.

The components at 1465 and 1455 cm^{-1} would correspond to true Lewis acid sites associated with the zeolite lattice itself. Such a duality of sites was reported by Cannings (*42*) in Na^+ mordenite leached with dilute sulfuric acid. He used a picture published by Uytterhoeven, Christner and Hall (*2*) in which the dehydroxylation mechanism is represented as:

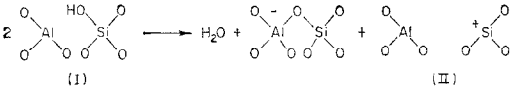

Structure (I) was associated with the weakest Lewis acid site (1455 cm^{-1}) and (II) with the strongest acid (1462 cm^{-1}) (*42*). This, however, cannot be true in Y zeolites, since the structure (I) does not take into account the coordination requirements of the aluminum for the oxygen (*10*). Structure (III) was proposed to give a more realistic representation of the hydroxyl sites, and Lewis centers are only created after dehydroxylation (*3*, *10*).

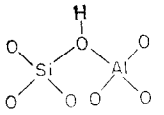

The existence of two types of Lewis sites is best understood in terms of dehydroxylated sites, for which structure (II) could be a more or less adequate picture,

at different points in the lattice, accessible to pyridine. Both Lewis pyridine bands are fully developed at 125°C. At that temperature only hydroxyls of the LF type were present. Dehydroxylation of these LF groups created two types of Lewis sites. This could be an indication that the LF OH band is heterogeneous and not due to a single well defined type of hydroxyls.

6. Decomposition Mechanisms

The primary alkylammonium derivatives generate a stoichiometric hydrogen Y zeolite. For each ion initially present, one OH group is generated. The simplest deamination reaction would be a reaction similar to that proposed in earlier studies for NH_4^+ zeolites (*1*, *2*, *4*):

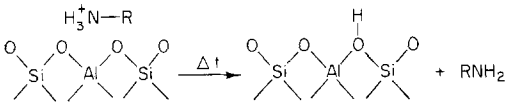

Below 350°C, the decomposition products of the B1 sample substantiate this reaction. For the M2 sample the same deamination reaction occurs below 350°C, but to a lower extent.

At higher temperatures the high amounts of NH_3 and butene detected suggest a Hofmann degradation of the butylammonium ion:

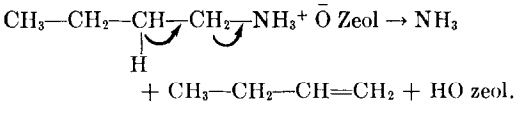

The formation of alkoxy groups on the zeolite, detected by IR spectroscopy, and the formation of NH_3 (sample B1) and methylamine (sample M2) suggest the following mechanisms:

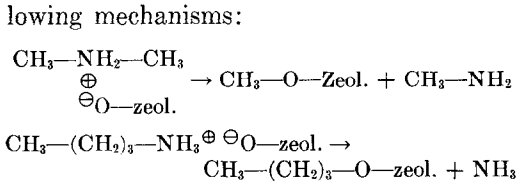

According to Wu, White and Venuto (*30*) the alkoxy species react at higher temperature by a hydride transfer mechanism. The reaction products of this reaction are CO, CO_2 and alkanes. The alkylammonium ions decomposed in this way do not produce a hydroxyl in the zeolite lattice. This mechanism could indeed occur in the sample M2: it would account for the decomposition products CO, CO_2, H_2 and especially CH_4, and also for the dehydroxylating effect on the zeolite. However, this mechanism is not likely to occur in the sample B1 since no butane is observed, and the zeolite is not dehydroxylated. Instead of this, the butoxy species could be eliminated by hydrolysis. The butanol molecules generated during this reaction could undergo an intermolecular hydride transfer with another alkoxy species as depicted by Wu *et al.* (*20*). This reaction pattern explains the presence of propane, H_2 and CO. Carbon dioxide can be accounted for by a water gas shift reaction between H_2O and CO. At high temperatures (460°C for M2) the nature of the reaction products NH_3, $CH_3—CH=CH_2$, $CH_2=CH_2$ suggests a mechanism closely related to the high temperature decomposition mechanism of tetramethylammonium Y proposed by Wu *et al.* (*20*). It includes ylide formation followed by intramolecular attack on ylide and Hofmann elimination.

The appearance of $(CH_3)_3N$ and CH_3NH_2 at 460°C suggests that a transalkylation reaction has occurred at lower temperatures:

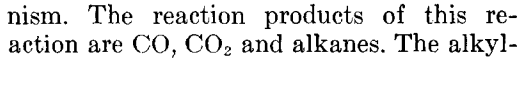

Such a mechanism was proposed by Fripiat, Durand and Pelet (*43*) for alkylammonium montmorillonites. These reactions occur below 300°C and are catalyzed by physically or chemically held water.

ACKNOWLEDGMENTS

One of us (P.J.) acknowledges a research grant from N.F.W.O. Belgium. The gift of the samples by Union Carbide Co. is appreciated. The technical assistance of Mrs. K. Rousseaux is acknowledged. We are indebted to Dr. Müller-Vonmoos for the DTA, TGA and mass spectrometric analysis. Suggestions and experimental help of Dr. B. K. G. Theng are gratefully acknowledged.

References

1. Rabo, J. A., Pickert, P. E., Stamires, D. N., and Boyle, J. E., *Actes Congr. Int. Catal., 2nd, 1960* **2**, 2055 (1961).
2. Uytterhoeven, J. B., Christner, L. G., and Hall, W. K., *J. Phys. Chem.* **69**, 2117 (1965).
3. Uytterhoeven, J. B., Jacobs, P., Makay, K., and Schoonheydt, R., *J. Phys. Chem.* **72**, 1768 (1968).
4. Ward, J. W., *J. Catal.* **9**, 225 (1967).
5. Bolton, A. P., and Lanewala, M. A., *J. Catal.* **18**, 154 (1970).
6. Basila, M. R., *Appl. Spectrosc. Rev.* **1**, 289 (1968).
7. Yates, D. J. C., *Catal. Rev.* **2**, 113 (1968).
8. Ward, J. W., *Int. Conf. Mol. Sieve Zeolites, 2nd, Worcester, 1970,* prepr. p. 682.
9. Eberly, P. E., Jr., *J. Phys. Chem.* **72**, 1042 (1968).
10. Olson, D. H., and Dempsey, E., *J. Catal.* **13**, 221 (1969).
11. Ward, J. W., *J. Phys. Chem.* **73**, 2086 (1969).
12. Wang, K. M., and Lunsford, J. H., *J. Phys. Chem.* **73**, 2069 (1969).
13. Kerr, G. T., *J. Catal.* **15**, 200 (1969).
14. Mc Daniel, C. V., and Maher, P. K., "Molecular Sieves," p. 186. Soc. Chem. Ind., London, 1968.
15. Hughes, T. R., and White, H. M., *J. Phys. Chem.* **71**, 2192 (1967).
16. White, J. L., Jelli, A. N., André, J. A., and Fripiat, J. J., *Trans. Faraday Soc.* **63**, 461 (1967).
17. Ward, J. W., *J. Catal.* **18**, 348 (1970).
18. Jacobs, P., and Uytterhoeven, J. B., *J. Catal.* **22**, 193 (1971).
19. Theng, B. K. G., Vansant, E., and Uytterhoeven, J. B., *Trans. Faraday Soc.* **64**, 3370 (1968).
20. Wu, E. L., Kühl, G. H., White, T. E., and Venuto, P. B., *Int. Conf. Mol. Sieve Zeolites, 2nd, Worcester, 1970,* prepr. p. 791.
21. Abramowitz, S., and Bauman, R. P., *J. Chem. Phys.* **39**, 2757 (1963).
22. Table 2, Ref. (*9*).
23. Cook, D., *Can. J. Chem.* **39**, 2009 (1961).
24. Katritzky, A. R., *J. Chem. Soc. (London)* 4162 (1958).
25. Parry, E. P., *J. Catal.* **2**, 371 (1963).
26. Basila, M. R., Kantner, T. R., and Rhee, K. H., *J. Phys. Chem.* **68**, 3197 (1964).
27. Schoonheydt, R. A., and Uytterhoeven, J. B., *J. Catal.* **19**, 55 (1970).
28. Ward, J. W., and Hansford, R. C., *J. Catal.* **13**, 364 (1969).
29. Liengme, B. V., and Hall, W. K., *Trans. Faraday Soc.* **62**, 3229 (1966).
30. Wu, E. L., White, T. E., and Venuto, P. B., *J. Catal.* **21**, 384 (1971).
31. Borello, E., Zecchina, A., and Monterra, D., *J. Phys. Chem.* **71**, 2938 (1967).
32. Greenler, R. G., *J. Chem. Phys.* **37**, 2094 (1962).
33. Sheppard, N., *in* "Hydrogen Bonding" (D. Hâdzi, ed.). Pergamon, Elmsford, NY, 1959.
34. Ramsay, D. A., *J. Amer. Chem. Soc.* **74**, 72 (1952).
35. Laby, R. H., and Walker, G. F., *J. Phys. Chem.* **74**, 2369 (1970).
36. Table 2, Ref. (*3*).
37. Taft, R. W., *in* "Steric effects in organic chemistry" (M. S. Newman, ed.), p. 556. Wiley, 1956.
38. Bertsch, L., and Habgood, H. W., *J. Phys. Chem.* **67**, 1621 (1963).
39. Ward, J. W., *J. Phys. Chem.* **72**, 4211 (1968).
40. Mortier, W., Bosmans, H., and Uytterhoeven, J. B., *J. Phys. Chem.* **76**, 650 (1972).
41. Gallezot, P., and Imelik, B., *C. R. Acad. Sci.* **271**, 912 (1970).
42. Cannings, F. R., *J. Phys. Chem.* **72**, 4691 (1968).
43. Durand, B., Pelet, R., and Fripiat, J. J., *Clays and Clay Miner.* **20**, 21 (1972).
44. Table 2, Ref. (*1*).